Article

Influence of Redox Molecules on the Electronic Conductance of Single-Walled Carbon Nanotube Field-Effect Transistors: Application to Chemical and Biological Sensing

Salah Boussaad, Bruce A. Diner, and Janine Fan

J. Am. Chem. Soc., **2008**, 130 (12), 3780-3787 • DOI: 10.1021/ja075131f

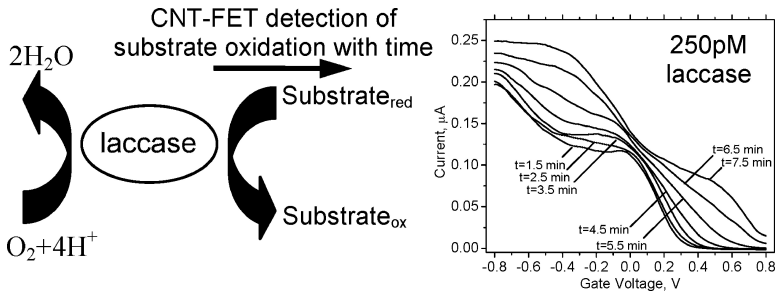

More About This Article

Additional resources and features associated with this article are available within the HTML version:

- Supporting Information
- Access to high resolution figures
- Links to articles and content related to this article
- Copyright permission to reproduce figures and/or text from this article

View the Full Text HTML

J|A|C|S
ARTICLES
Published on Web 03/06/2008

Influence of Redox Molecules on the Electronic Conductance of Single-Walled Carbon Nanotube Field-Effect Transistors: Application to Chemical and Biological Sensing

Salah Boussaad, Bruce A. Diner,* and Janine Fan

Central Research and Development, Experimental Station, E. I. du Pont de Nemours & Co, Wilmington, Delaware 19880-0173

Received July 10, 2007; E-mail: bruce.a.diner@usa.dupont.com

Abstract: In an effort to develop sensitive nanoscale devices for chemical and biological sensing, we have examined, using liquid gating, the conductance of semiconducting single-walled carbon nanotube-based field-effect transistors (SWCNT-FETs) in the presence of redox mediators. As examples, redox couples $K_3Fe(CN)_6/K_4Fe(CN)_6$ and K_2IrCl_6/K_3IrCl_6 are shown to modulate the SWCNT-FET conductance in part through their influence via the electrolyte gate on the electrostatic potential of the solution, as described by Larrimore et al. (*Nano Lett.* **2006**, *6*, 3129−1333) and in part through electron transfer between the redox mediators and the nanotubes. In the latter case, the rate of electron transfer is determined by the difference in chemical potential between the redox mediator and the SWCNTs and by the concentrations of the oxidized and reduced forms of the redox couple. Furthermore, these devices can detect the activity of redox enzymes through their sensitivity to the change in oxidation state of the enzyme substrate. An example is given for the blue copper oxidase, *Trametes versicolor* laccase, in which the rate of change of the SWCNT device conductance is linearly proportional to the rate of oxidation of the substrate 10-(2-hydroxyethyl)phenoxazine, varied over 2 orders of magnitude by the laccase concentration in the picomolar range. The behavior described in this work provides a highly sensitive means with which to do chemical and biological sensing using SWCNTs that is different from the amperometric, capacitive, and field-effect type sensing methods previously described in the literature for this material.

Introduction

Carbon nanotubes[1−5] display physical and electronic properties that are particularly amenable to use in miniature devices for chemical sensing. Single-walled carbon nanotubes (SWCNTs) are rolled-up one-atom-thick graphene sheets with diameters on the nanometer scale. Depending on their chirality, they can show metallic or semiconducting behavior, with the latter able to act as field-effect transistors (FETs).[6] It is known that bare SWCNTs are sensitive to their chemical environment, specifically exposure to air or to oxygen[4,7] and to other molecules such as NO_2 or NH_3,[8] which alter their electronic properties, permitting them to act as chemical gas sensors. When coated with selective polymers or metal nanoparticles, their range as gas sensors can be extended to CO_2[9]and to H_2, CH_4, CO, and H_2S,[10] respectively. Bare SWCNTs are also sensitive to their redox environment as indicated by the influence of aqueous solutions of oxidants and reductants, on the nanotube absorbance spectra.[11−13] The redox mediators are in electrochemical equilibrium with dispersed carbon nanotubes such that the occupancy of the electronic states of the valence band can be varied reversibly.[11,12]

Krüger et al.[14] and Rosenblatt et al.[15] have shown that SWCNT-based field-effect transistors (FETs) can be electrolytically gated with high sensitivity. We have been examining such electrolytic gating of SWCNT-FETs in the presence of redox mediators in an effort to understand the consequences for electronics of the reversible oxidation and reduction revealed by the earlier spectroscopic redox studies[11,12] and to apply such electrochemical redox sensing to the detection of biomolecules.[16] A schematic view of the SWCNT devices used is shown in Figure 1A. Here the source (S) and drain (D) electrodes are bridged by semiconducting SWCNTs, with the conductivity of

(1) Iijima, S. *Nature* **1991**, *354*, 56−8.
(2) Dresselhaus, M. S.; Dresselhaus, G.; Avouris, P. *Carbon Nanotubes Synthesis, Structure, Properties, and Applications*; Springer-Verlag: Berlin, 2001; pp 447.
(3) Odom, T. W.; Huang, J.-L.; Kim, P.; Lieber, C. M. *J. Phys. Chem. B* **2000**, *104*, 2794−2809.
(4) Avouris, P. *Chem. Phys.* **2002**, *281*, 429−445.
(5) Dai, H. *Acc. Chem. Res.* **2002**, *35*, 1035−1044.
(6) Tans, S. J.; Verschueren, A. R. M.; Dekker, C. *Nature* **1998**, *393*, 49−52.
(7) Collins, P. G.; Bradley, K.; Ishigami, M.; Zettl, A. *Science* **2000**, *287*, 1801−1804.
(8) Kong, J.; Franklin, N. R.; Zhou, C.; Chapline, M. G.; Peng, S.; Cho, K.; Dai, H. *Science* **2000**, *287*, 622−625.
(9) Star, A.; Han, T.-R.; Joshi, V.; Gabriel, J.-C. P. *Adv. Mater.* **2004**, *16*, 2049−2052.
(10) Star, A.; Tu, E.; Niemann, J.; Gabriel, J.-C. P.; Joiner, C. S.; Valcke, C. *Proc. Natl. Acad. Sci. U.S.A.* **2006**, *103* (4), 921−926.
(11) Zheng, M.; Diner, B. A. *J. Am. Chem. Soc.* **2004**, *126*, 15490−15494.
(12) Li, L.-J.; Nicholas, R. J. *Nanotechnology* **2004**, *15*, 1844−1847.
(13) Barone, P. W.; Baik, S.; Heller, D. A.; Strano, M. S. *Nat. Mater.* **2005**, *4*, 86−92.
(14) Kruger, M.; Buitelaar, M. R.; Nussbaumer, T.; Schonenberger, C.; Forro, L. *Appl. Phys. Lett.* **2001**, *78*, 1291−1293.
(15) Rosenblatt, S.; Yaish, Y.; Park, J.; Gore, J.; Sazonova, V.; McEuen, P. L. *Nano Lett.* **2002**, *2*, 869−872.
(16) Boussaad, S.; Diner, B. A.; Fan, J.; Rostovtsev, V. Redox potential mediated, heterogeneous, carbon nanotube biosensing. PCT/ US2005/03562 (WO2007/001402).

10.1021/ja075131f CCC: $40.75

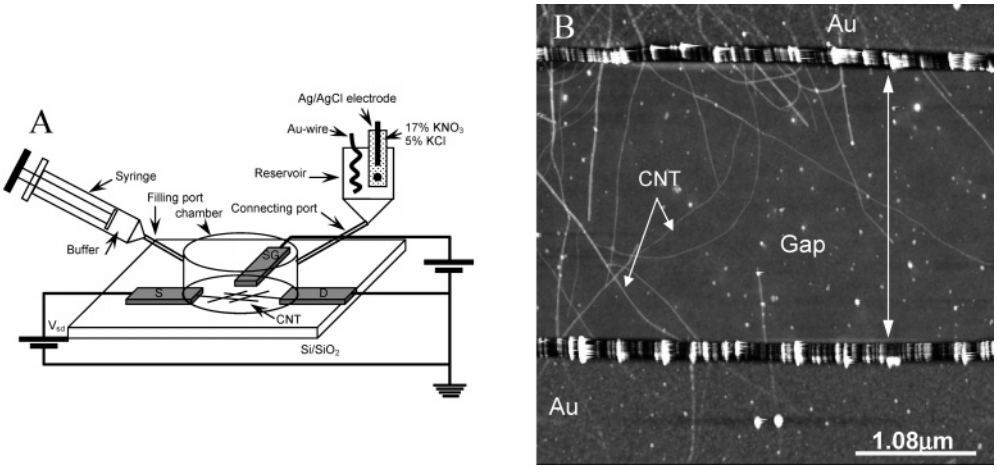

Figure 1. (A) Schematic of single-walled carbon nanotube-based field-effect transistor. The source (S), drain (D), and surface gate (SG) electrodes are lithographically patterned on the surface of a Si/SiO_2 chip, with the first two bridged by previously grown chemical vapor deposition (CVD) carbon nanotubes. An electrolyte/buffer chamber sealed by an O-ring is clamped to the surface and contains a 4.4. μL volume which is in contact with the three electrodes. Connected to the chamber through the filling and connecting ports is, respectively, a syringe containing electrolyte/buffer solution and an electrolyte/buffer-filled reservoir in which is immersed a 50 μm coiled gold wire and a Ag/AgCl electrode (ThermOrion 97-78-00) bathed in 17% KNO_3 + 5% KCl and connected to the external electrolyte/buffer solution through a porous frit. A gate voltage (V_g versus ground) is applied to any one of the three gate electrodes during which time the source-drain current (I_{sd}) is measured while applying a 50 mV bias (V_{sd}). (B) AFM image of the 2 μm gap of the SWCNT-FET between gold electrodes at upper and lower edges.

the latter modulated by a variety of gate electrodes immersed in the same electrolyte solution as the nanotubes. The location of the gate electrodes is either on the same chip surface as the SWCNT-FETs (gold electrode, SG) or in a reservoir electrolytically linked to the chamber containing the SWCNT-FETs (gold wire, Ag/AgCl electrode). Larrimore et al.[17] have recently reported, in similar such devices, a sensitivity of the nanotube conductance to the electrostatic potential of the solution, as determined by the chemical potential of the redox couple interacting with the gate electrode. The applied gate voltage, V_g, clamps the electrochemical potential of the solution and is equal to the sum of the electrostatic potential of the solution (φ) and the chemical potential of the electrons (μ/e) of the dissolved redox couple as expressed by the Nernst equation.

$$V_g = \frac{\bar{\mu}}{e} = \varphi + \frac{\mu}{e} = \varphi + E^{0'} + \frac{kT}{ne}\ln\frac{[Ox]}{[Red]} \qquad (1)$$

Under the conditions of their experiments, the nanotube acts as a reference electrode, sensing primarily changes in the electrostatic potential of the solution and not to a significant extent electron transfer between the nanotube and the redox mediator.

We[11] and others[12] have recently shown through UV/vis/NIR spectroscopy that dispersed SWCNTs can be reversibly oxidized and reduced using redox mediators in aqueous solution. Oxidation results in the bleaching of the E11 optical transitions with the longer wavelength absorbing nanotubes (i.e., smaller band gap, larger diameter) undergoing oxidation at lower redox potentials than those absorbing to shorter wavelength (see also refs 13, 18). The smaller the band gap, the higher the energy of the valence band and the smaller the work function for electron extraction.[18] Oxidation of the SWCNTs implies an emptying of the electronic states in the valence band (an increase in the concentration of p-type charge carriers), leading one to expect that such oxidation should result in increased p-type conductance with increasing redox potential. Net electron transfer between the nanotubes and the redox mediators should also occur in SWCNT-FETs under conditions of electrochemical gating. Indeed, in a recent theoretical paper, Heller et al.[19] argue that a potential difference applied between a SWCNT and the electrolyte solution in which it is immersed changes the chemical potential of the nanotube, driving electron transfer between a redox mediator in solution and the nanotube. Experiments that we have carried out over the last 3 years[16] support this view. This behavior provides, in addition to that reported by Larrimore et al.,[17] a new route to chemical and biological sensing using SWCNTs that is different from the amperometric,[20−23] capacitive,[24] and field-effect type sensing[10,25,26] methods previously described.

Materials and Methods

Single-Walled Carbon Nanotube FETs. SWCNTs were grown on Si/SiO_2 wafers by CVD from catalyst islands atop a 500 nm thick oxide layer (Molecular Nanosystems Inc.). The islands were overlaid with titanium (<5 nm), palladium (~25 nm), and gold (~25 nm) to form electrodes 12 μm on edge with 2 μm gaps which were extended to 300 μm^2 pads toward the edges of the chips for contacting with probes. The wafer was then diced into chips 11 mm^2. The source-drain currents (I_{sd}) vs V_g of the devices were first characterized in air. The metallic nanotubes that bridge the gap were selectively destroyed in air[4,27] by ramping the bias voltage (V_{sd}) from 0 to 10 V with V_g of the silicon backgate set to 0 V, which resulted in enhancing the I_{sd} on/off ratio of

(17) Larrimore, L.; Nad, S.; Zhou, X.; Abruna, H.; McEuen, P. L. *Nano Lett.* **2006**, *6*, 1329−1333.
(18) Okazaki, K.-i.; Nakato, Y.; Murakoshi, K. *Phys. Rev. B* **2003**, *68*, 035434/1−035434/5.
(19) Heller, I.; Kong, J.; Williams, K. A.; Dekker, C.; Lemay, S. G. *J. Am. Chem. Soc.* **2006**, *128*, 7353−7359.
(20) Wang, J. *Electroanalysis* **2005**, *17*, 7−14.
(21) Napier, M. E.; Hull, D. O.; Thorp, H. H. *J. Am. Chem. Soc.* **2005**, *127*, 11952−11953.
(22) Guiseppi-Elie, A.; Lei, C.; Baughman, R. H. *Nanotechnology* **2002**, *13*, 559−564.
(23) Li, J.; Ng, H. T.; Cassell, A.; Fan, W.; Chen, H.; Ye, Q.; Koehne, J.; Han, J.; Meyyappan, M. *Nano Lett.* **2003**, *3*, 597−602.
(24) Snow, E. S.; Perkins, F. K.; Houser, E. J.; Badescu, S. C.; Reinecke, T. L. *Science* **2005**, *307*, 1942−1945.
(25) Star, A.; Gabriel, J.-C. P.; Bradley, K.; Gruener, G. *Nano Lett.* **2003**, *3*, 459−463.
(26) Chen, R. J.; Bangsaruntip, S.; Drouvalakis, K. A.; Kam, N. W. S.; Shim, M.; Li, Y.; Kim, W.; Utz, P. J.; Dai, H. *Proc. Natl. Acad. Sci. U.S.A.* **2003**, *100*, 4984−4989.
(27) Collins, P. G.; Arnold, M. S.; Avouris, P. *Science* **2001**, *292*, 706−9.

the devices from 2 to 3 to 10^3-10^4. The number of nanotubes that completely bridge the gap typically range from 3 to 6, which means that even with destruction of the metallic nanotubes there are multiple pathways with one or more semiconducting nanotubes for conduction involving nanotubes of different chirality. The chips were then clamped onto a copper plate using an O-ring-sealed flow cell which allowed syringe-driven flow of electrolyte/buffer solution through a filling port into a 4.4 μL chamber containing the carbon nanotube devices. The electrolye/buffer flowed through a connecting port to a reservoir containing a gold wire and a Ag/AgCl electrode, bathed in 17% KNO_3 + 5% KCl solution and making electrolytic contact with the external electrolyte/buffer through a porous frit. Both of these electrodes were used independently as gate electrodes and were $\gg$1000 times the surface area of the source and drain electrodes bridged by the nanotubes. A third independent gate electrode (SG), lying on the chip surface, had the same dimensions as the source and drain electrodes. The I_{sd} vs V_g sweeps were controlled using an Agilent Model E5270B precision source monitor unit, configured with three independent channels dedicated to the source, drain, and gate. The source-drain bias was set at 50 mV and the gate voltage swept from negative to positive V_g in 45 s, for each of the above-mentioned gate electrodes as indicated in the figure legends. The leakage currents between the gate and the drain electrode were measured during the course of the V_g sweeps. All measurements were made with the flow stopped, following incubation with the redox couple for at least 10 min, except for time course experiments where the incubation times were as indicated. The I_{sd} vs V_g plots were smoothed by adjacent averaging with windows of 10 points out of a total of 250 data points.

Each experimental condition was routinely examined using the same gate but two or three different source/drain electrode pairs on the same chip. While the saturating currents would vary (typically within a factor of 2, though occasionally a factor 3) owing to variation in the number of nanotubes bridging the electrodes, the behavior was quantitatively the same when normalized to the saturating current of each device.

Measurements of the solution redox potential were made using the combination redox electrode (97−78-00 ThermOrion), the Ag/AgCl component of which was used as a gate electrode.

Laccase. Two grams of crude *Trametes versicolor* laccase (a gift of Wacker Chemie) were purified by washing with 20 mM Bis-tris propane pH 6.0 using a YM-30 membrane in an Amicon ultrafiltration cell (Millipore). The concentrated washed enzyme was then purified on a G2000SW gel filtration column (2.15 cm ID × 60 cm, TosoHaas) using 50 mM Na acetate pH 5.0 plus 0.1 M Na_2SO_4 at 5.0 mL/min. Typical recovery was 65−95 mg protein at a specific activity of 8−9 OD/min per μg protein/mL at 436 nm using as substrate 5 mM ABTS (2,2′-azinobis(3-ethylbenzthiazolinesulfonate) in 50 mM glycine pH 3.0.

Results

Optical Response to $K_3Fe(CN)_6/K_4Fe(CN)_6$. In our earlier work,[11] the high potential oxidants, K_2IrCl_6 (E_m = 867mV vs NHE)[28] and $KMnO_4$ (E_m = 1.51 V vs NHE), were shown to oxidize SWCNTs with a broad range of chiralities. It is also possible to use weaker oxidants such as $K_3Fe(CN)_6$ (E_m = 356 mV vs NHE),[29,12,13] though the extent of oxidation is more limited and is restricted to those nanotubes with smaller bandgaps. An example of the action of this redox reagent is shown in Figure 2. The addition of $K_3Fe(CN)_6$ to an aqueous suspension of detergent-dispersed HiPco carbon nanotubes (Carbon Nanotechnologies Inc.) produces a time-dependent bleaching of the E11 optical transitions (Figure 2A,B). As previously shown with K_2IrCl_6 and with $K_3Fe(CN)_6$, those

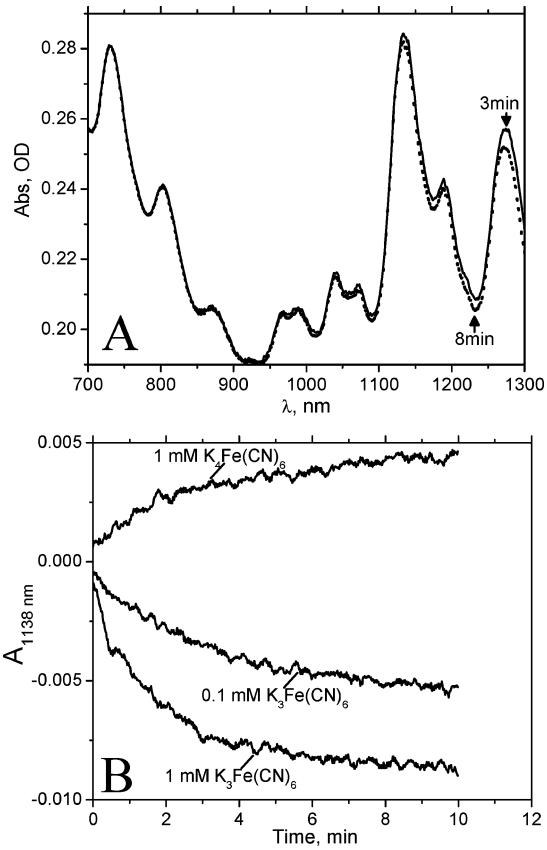

Figure 2. Absorbance spectra of HiPco carbon nanotubes. (A) Measurements at 3 min and 8 min after the addition of 1 mM $K_3Fe(CN)_6$ in 50 mM glycine pH 9.0. (B). Time course of the change of absorbance at 1138 nm, following the addition of 0.1 and 1 mM $K_3Fe(CN)_6$ and 1 mM $K_4Fe(CN)_6$ in 50 mM glycine pH 9.0.

nanotubes absorbing at longer wavelength undergo greater bleaching than those at shorter wavelength. In addition, there is a shift of the absorbance maximum to shorter wavelength. Both observations stem from the preferential oxidation of the nanotubes with smaller band gap (larger diameter) at a given redox potential.[13,18] A plot of this bleaching with time for the optical transition at 1138 nm is shown in Figure 2B, where the rate of absorbance decrease on the minutes time scale is dependent on the mediator concentration, increasing with higher $K_3Fe(CN)_6$ concentration. Interestingly, the addition of $K_4Fe(CN)_6$ produces an absorbance change in the opposite direction, an increase in absorbance that reflects a reductive process. This observation implies that the nanotube suspension was partially oxidized by O_2 even before the addition of the redox reagent[11] and so is reduced by the addition of the reduced form of the mediator.

Electronic Response to $K_3Fe(CN)_6/K_4Fe(CN)_6$. We first examined the effect of $K_4Fe(CN)_6$ and $K_3Fe(CN)_6$ to better understand the implications of the solution optical behavior of the SWCNTs on the electronic properties of the SWCNT-FET.

The SWCNT-FETs were electrochemically gated using three different gate electrodes for reasons that are detailed below. The surface gate (SG, Figures 1A, 3A), with dimensions similar to those of the source and drain electrodes, was initially chosen as it appeared to be best adapted to the inclusion of all of the electrodes within a microfluidic channel for nanoscale chemical and biological sensing. In this case, the potential difference between the gate and the source/drain electrodes drops partially

(28) Dean, J. A.; Lange, N. A. *Lange's Handbook of Chemistry*, 5th ed.; McGraw-Hill: New York, 1999.
(29) Winefordner, J. D.; Davison, G. A. *Anal. Chim. Acta* **1963**, *28*, 480−94.

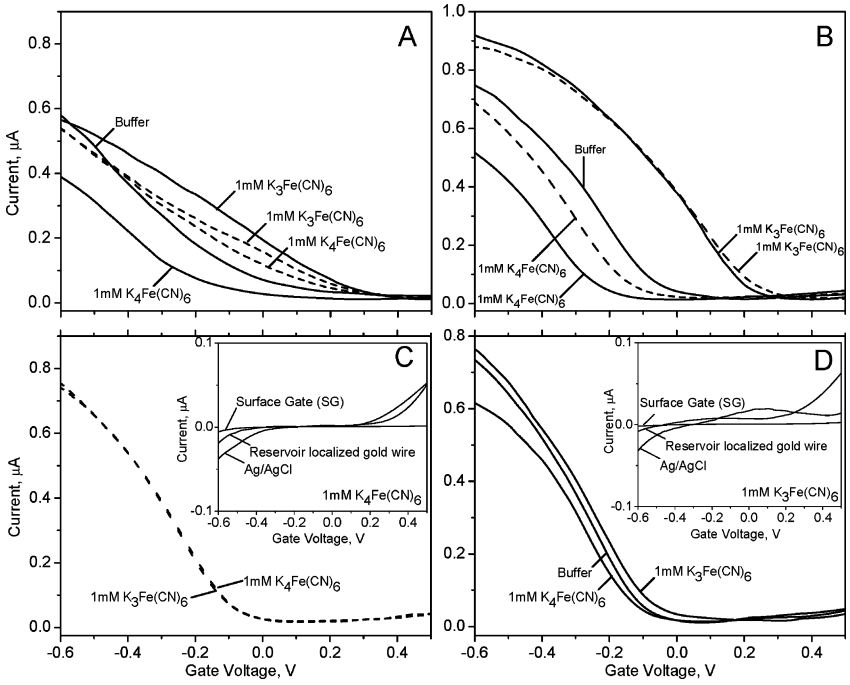

Figure 3. I_{sd} versus V_g in the presence of $K_3Fe(CN)_6$ and $K_4Fe(CN)_6$ using as gate electrodes the surface gate, SG (A), and the reservoir-localized gold wire (B) and the reservoir-localized Ag/AgCl reference electrode (C and D). All measurements were performed in the presence of 50 mM glycine pH 9.0 in the chamber and reservoir. The dashed lines show I_{sd} vs V_g with the redox mediators confined to the reservoir. The solid curves were recorded with the redox mediators located throughout and after 10 min of incubation. The curves marked "buffer" contain no redox mediator. The leakage current measured between the gate and the drain electrode has been subtracted. V_g was swept from −0.8 to +0.8 V in 45 s. V_{sd} = 50 mV. Inset 3C: Leakage current measured between the indicated gate electrode and the drain electrode in the presence of 1 mM $K_4Fe(CN)_6$. Inset 3D: Leakage current measured between the indicated gate electrode and the drain electrode in the presence of 1 mM $K_3Fe(CN)_6$.

and to a similar extent at both the gate/liquid and the source-drain-nanotube/liquid interface. The gold wire in the reservoir (Figure 3B) has about 3000 times the surface area of the source and drain electrodes. In this case, the potential difference between the gate and the source-drain electrodes drops primarily at the source-drain-nanotube/liquid interface. Figures 3A and 3B show the I_{sd} vs V_g response of the SWCNT devices to buffer alone and to buffer containing 1 mM $K_4Fe(CN)_6$ and 1 mM $K_3Fe(CN)_6$. The redox mediators were either confined to the reservoir (dashed lines) or present in both the chamber and the reservoir (solid lines). In the latter case, the buffer containing the redox mediator was allowed to flow through the chamber after which it was allowed to remain in contact with the SWCNT-FETs for 10 min prior to the start of the measurement. Figures 3A and 3B show that contact of the SWCNT-FETs with 1 mM $K_4Fe(CN)_6$ shifts the I_{sd} vs V_g curves such that the turn-on voltage is shifted negative relative to the buffer alone, while contact with 1 mM $K_3Fe(CN)_6$ shifts the curves in the opposite direction. In Figure 3A, $K_4Fe(CN)_6$ and $K_3Fe(CN)_6$, have, as expected, virtually no influence on the SWCNT-FETs when the redox mediators are confined to the reservoir (dashed lines) and not in contact with electrodes S, D and SG. However, in Figure 3B, the I_{sd} vs V_g curves shift substantially when the redox mediators are confined to the reservoir but in contact with the gold wire gate electrode. This influence of the redox mediators on the I_{sd} vs V_g curves when in contact with the gate electrode only is consistent with the observations of Larrimore et al.,[17] where the threshold voltage shift of the SWCNT-FETs is equivalent to the change in the chemical potential of the solution, a total difference of approximately 220 mV (the redox potential difference between the 1 mM $K_3Fe(CN)_6$ and 1 mM $K_4Fe(CN)_6$ solutions). A marked additional shift to negative V_g is, however, observed in Figure 3B, for 1 mM $K_4Fe(CN)_6$, when the redox mediator solution is in direct contact with the SWCNT-FETs compared to the reservoir only case.

The influence of 1 mM $K_4Fe(CN)_6$ on the SWCNT-FETs was examined further using as gate the Ag/AgCl reference electrode in the reservoir. This electrode, which is isolated by a salt bridge from the electrolyte solution, and therefore from the redox couple, clamps only the electrostatic potential of the solution. Consistent with this picture, Figure 3C shows no displacement of the I_{sd} vs V_g when either 1 mM $K_3Fe(CN)_6$ and 1 mM $K_4Fe(CN)_6$ are confined to the reservoir. If there were no electron transfer between the SWCNT-FETs and the redox mediators, then similar curves should be observed when the SWCNT-FETs are in contact with the redox mediators. It is clear in Figure 3D, at least in the case of 1 mM $K_4Fe(CN)_6$, that I_{sd} deviates increasingly from the buffer trace as V_g becomes increasingly negative, with a lower saturating current relative to that observed when the mediator is confined to the reservoir (Figure 3C). This observation is consistent with the additional shift observed in Figure 3B when 1 mM $K_4Fe(CN)_6$ is brought into contact with the SWCNT-FET. This observation can be explained by a lowering of the Fermi level relative to the energy of the valence band as V_g becomes increasingly negative, resulting in an increased number of vacant electronic states that are capable of accepting electrons from $K_4Fe(CN)_6$. As the SWCNT-FET current is a reflection of the concentration of p-type charge carriers in the nanotubes, electron transfer from $K_4Fe(CN)_6$ to the nanotubes decreases the concentration of charge carriers, relative to what is observed in the absence of the redox mediator, lowering the observed current at a given V_g. Similar behavior was consistently observed in at least ten different devices.

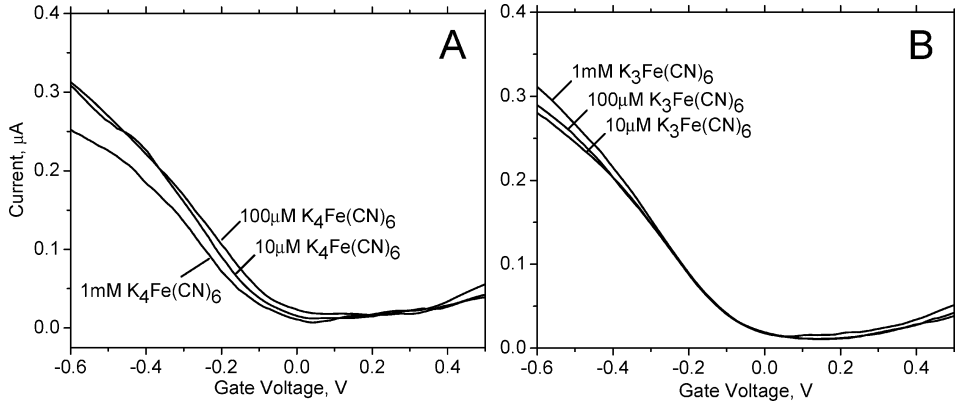

Figure 4. I_{sd} vs V_g using as gate the Ag/AgCl reference electrode placed in the reservoir. (A) Measurements after 10 min incubation in the presence of the indicated concentrations of $K_4Fe(CN)_6$ in 50 mM glycine pH 9.0 and present in both the chamber and reservoir. (B) Measurements after 10 min incubation in the presence of the indicated concentrations of $K_3Fe(CN)_6$ in 50 mM glycine pH 9.0 and present in both the chamber and reservoir. The leakage current measured between the gate and the drain electrode has been subtracted. V_g was swept from −0.8 to +0.8 V in 45 s. V_{sd} = 50 mV.

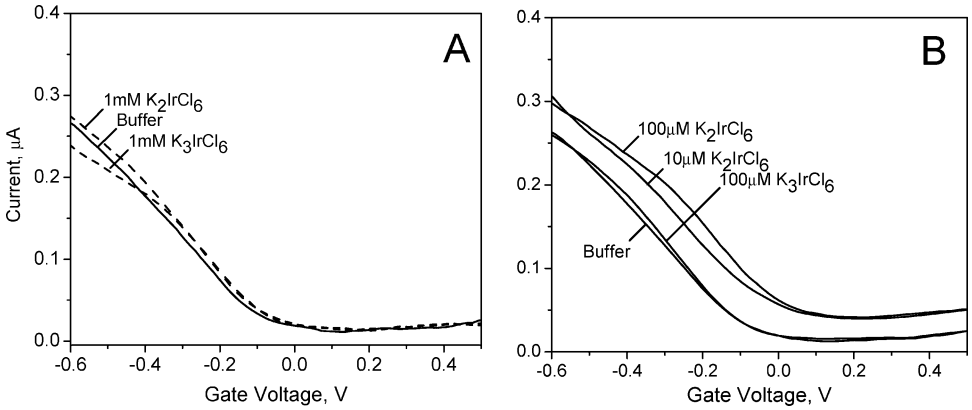

Figure 5. Figure 5. I_{sd} vs V_g in the presence of K_2IrCl_6 and K_3IrCl_6 using as gate the reservoir-localized Ag/AgCl electrode. (A) with the redox solutions restricted to the reservoir. (B) with the redox solution present in both the reservoir and the chamber and after a 10 min incubation at the indicated concentrations of K_2IrCl_6 and K_3IrCl_6. All measurements were performed in the presence of 50 mM glycine, pH 9.0, in the chamber and reservoir. The leakage current measured between the gate and the drain electrode has been subtracted. V_g was swept from −0.8 to +0.8 V in 45 s. V_{sd} = 50 mV.

If indeed there were electron transfer between the redox mediator and the nanotubes of the SWCNT-FET, modulated by device gating, then the extent to which the current of the devices were lowered by $K_4Fe(CN)_6$ should depend on the flux of mediator to the nanotube, proportional to the mediator concentration. Figure 4A shows, using the Ag/AgCl reservoir-localized gate electrode, that as the concentration of the $K_4Fe(CN)_6$ in contact with the device is lowered from 1 mM, the suppression of I_{sd} by the mediator at negative V_g decreases and approaches a limit (∼100 μM) below which the concentration of the mediator no longer has any influence. $K_3Fe(CN)_6$ has a smaller influence on I_{sd} vs V_g but opposite in sign to that of $K_4Fe(CN)_6$, producing only a small increase in current which is more pronounced at higher concentration. These observations are consistent with the optical changes observed in Figure 2B, which reflect electron transfer to and from the nanotubes by reduction and oxidation of the nanotubes by $K_4Fe(CN)_6$ and $K_3Fe(CN)_6$, respectively.

Electronic Response to K_2IrCl_6/K_3IrCl_6. The ferri/ferrocyanide redox couple has over the pH range from 4.0 to 9.0 a reduction potential (E^0 = 0.356 V vs NHE[29]) capable of only modest oxidation of SWCNTs (e.g., Figure 1). It was previously shown[11] that K_2IrCl_6 (E_m = 0.867 V[28] for redox couple K_2IrCl_6/K_3IrCl_6) is capable of nearly complete oxidation of (6,5) nanotubes (E_m ∼ 0.80 V). Figure 5A shows the absence of any influence of 1 mM K_3IrCl_6 andK_2IrCl_6 on device conductance when restricted to the reservoir alone with Ag/AgCl as the gate electrode. Incubation of the reservoir and chamber with 1 mM K_3IrCl_6 and using the same SWCNT-FET device as in Figure 4 resulted in a much more limited influence on the SWCNT-FET conductance than was observed with 1 mM $K_4Fe(CN)_6$, consistent with the much less favorable reduction potential for K_3IrCl_6 oxidation. However, incubation of the reservoir and chamber with 100 μM K_2IrCl_6 produced a substantial positive shift of the threshold voltage and a large increase in conductance over the entire range of V_g, far greater than the minor effect observed with $K_3Fe(CN)_6$. The effect is larger still with 1 mM K_2IrCl_6 (not shown), but, at this concentration, there is a substantial leakage current. A small further decrease in I_{sd} is observed upon replacement of 100 μM with 10 μM K_2IrCl_6. This much greater effect on I_{sd} of K_2IrCl_6 than for $K_3Fe(CN)_6$ is consistent with its much more positive reduction potential and the near quantitative oxidation of the (6,5) SWCNTs observed earlier.[11]

Electronic Sensing of Laccase Activity. The sensitivity of the SWCNT-FET conductance to the presence of redox mediators offers the possibility of sensing redox enzymes, the activity of which would be detected by measuring the rate of change in chemical potential of a solution of redox active substrate. *Trametes versicolor* laccase, a blue copper oxidase containing four coppers per monomer, catalyzes the oxidation of a broad range of phenols and arylamines at the expense of molecular

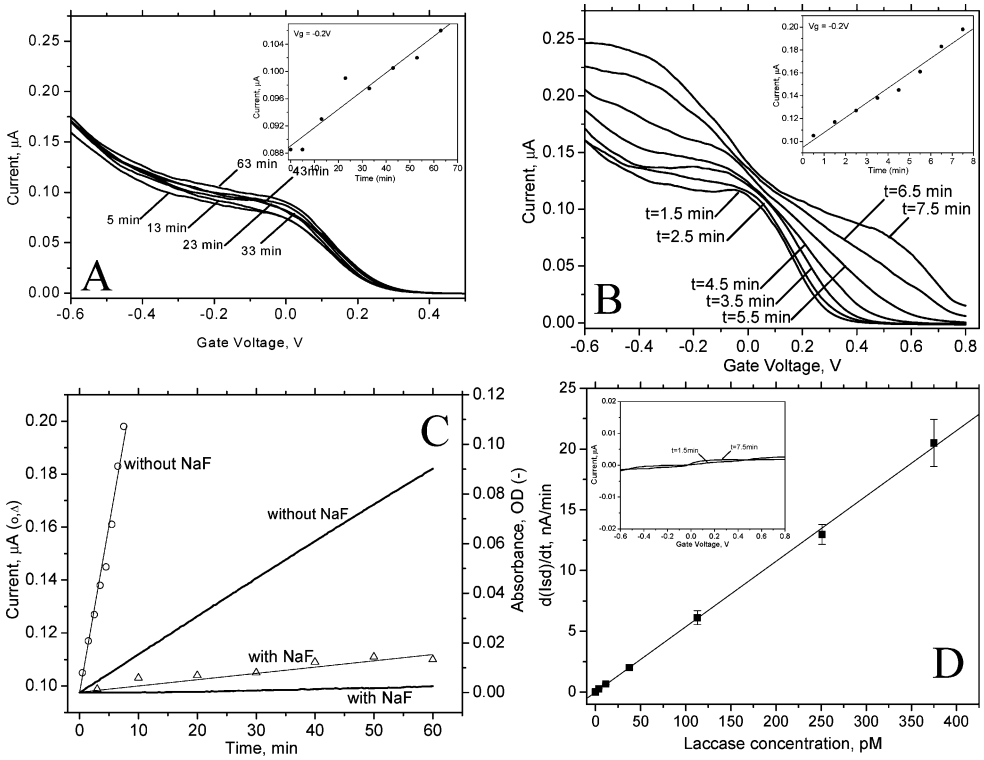

Figure 6. Plots of I_{sd} versus V_g at different laccase concentrations. (A) Measurements as a function of time in the presence of 3.75 pM laccase and 22 μM 10-(2-hydroxyethyl)phenoxazine in 25 mM glycine pH 4.0. $V_{sd} = 50$ mV. Inset: plot of I_{sd} at $V_g = -0.2$ V as a function of time. (B) Measurements as a function of time in the presence of 250 pM laccase and 22 μM 10-(2-hydroxyethyl)phenoxazine in the presence of 25 mM glycine pH 4.0. Inset: plot of I_{sd} at $V_g = -0.2$ V as a function of time. For A and B, V_g was swept from -0.8 to $+0.8$ V in 45 s. $V_{sd} = 50$ mV. (C) Thin lines: I_{sd} measured as a function of time under the same conditions as in Figure 6B in the presence (△) and absence (○) of 1 mM NaF. Thick lines: Absorbance at 528 nm as a function of time in the presence 500 pM and 22 μM 10-(2-hydroxyethyl)phenoxazine in 25 mM glycine pH 4.0. (D) Rate of change of I_{sd} at $V_g = -0.2$V with time as a function of the laccase concentration, measured as in the insets of Figures 6A and 6B. Inset: Leakage current between the SG gate and the drain electrode at 1.5 and 7 min after the start of oxidation of 10-(2-hydroxyethyl)phenoxazine by 250 pM laccase.

oxygen, which is reduced to water.[30] One of the highest affinity substrates for laccase is 10-(2-hydroxyethyl)phenoxazine, which has been reported to have at pH 5.3 a reduction potential vs NHE of 772.6 ± 3.2 mV, a K_m of 5.9 ± 0.7 mM and a k_{cat} of 120 ± 4 s^{-1}.[31]

Detection of enzyme activity is demonstrated in Figures 6A and 6B which shows the evolution of the I_{sd} versus V_g plots as a function of time for 3.75 and 250 pM enzyme, respectively, in the presence of 22 μM 10-(2-hydroxyethyl)phenoxazine in 25 mM glycine buffer, pH 4.0. The basis of the sensing is that the SWCNT devices respond much more rapidly to a change in redox state of the 10-(2-hydroxyethyl)phenoxazine than they do to the concentration of oxygen. NaF is an inhibitor of laccase, thought to be acting at the Type-2 copper center.[32] Figure 6C shows both colorimetrically and electronically that the addition of 1 mM NaF to 500 and 250 pM laccase, respectively, in 25 mM glycine, pH 4.0, containing 22 μM 10-(2-hydroxyethyl)-phenoxazine slows the enzyme reaction by close to 50-fold. A series of I_{sd} vs V_g measurements were conducted at concentrations of laccase varying from 3.75 to 375 pM in the presence of 22 μM 10-(2-hydroxyethyl)phenoxazine in 25 mM glycine pH 4.0. Plots of the variation of the nanotube device current at $V_g = -0.20$ V in the presence of 3.75 and 250 pM laccase (Figures 6A and 6B insets, respectively) show the evolution of the current, associated with 10-(2-hydroxyethyl)phenoxazine oxidation, to be linear with time. The noise level of the slope measurement in Figure 6A inset corresponds to a concentration uncertainty on the order of ±0.4 pM. A plot of the slope of the rate of change of the current with time versus the laccase concentration shows the slope to be a linear indicator of laccase concentration over a range of 2 orders of magnitude (Figure 6D).

Discussion

The gold wire electrode used as gate in the reservoir senses the solution electrochemical potential which is composed of the electrostatic potential of the solution and the chemical potential of the redox mediator (see eq 1). Larrimore et al.[17] have argued, using an experimental arrangement similar to that used here, that the SWCNT-FET is primarily a sensor of the electrostatic potential of the solution, where the shift in the position of the I_{sd} vs V_g curves along the V_g axis is caused by a change in the solution electrostatic potential, produced by electron transfer between the redox couple and the gate electrode. The extent of the change in electrostatic potential is equal to the change in the redox potential of the redox couple. The observations of Larrimore et al.[17] for the case where the redox mediator is confined to the reservoir alone are confirmed in Figure 3B. One millimolar $K_3Fe(CN)_6$ and 1 mM $K_4Fe(CN)_6$ produce an approximate 220 mV difference of the I_{sd} vs V_g curves relative to each other when the redox mediator is in contact with the

(30) Bertrand, T.; Jolivalt, C.; Briozzo, P.; Caminade, E.; Joly, N.; Madzak, C.; Mougin, C. *Biochemistry* **2002**, *41* (23), 7325−7333.
(31) Kulys, J.; Krikstopaitis, K.; Ziemys, A. *J. Biol. Inorg. Chem.* **2000**, *5*, 333−340.
(32) Reinhammar, B. *Laccase in Copper Proteins and Copper Enzymes*; Lonti, R., Ed.; CRC: Boca Raton, 1984; pp 1−35.

reservoir-localized gold wire gate electrode only and not in direct contact with the SWCNT-FETs. Unlike the gold wire electrode, the Ag/AgCl electrode cannot undergo electron transfer with the mediator. It cannot sense the chemical potential of the redox couple, and it fixes the solution electrostatic potential only. Consequently, changes in the redox potential of the reservoir solution produce no displacement in the I_{sd} vs V_g when this electrode is used as the gate (see Figures 3C and 5A). Were the SWCNT-FET to sense the solution electrostatic potential only, then there should be virtually no difference between the I_{sd} vs V_g curves where the redox mediator is confined to the reservoir and where it is in contact with both the reservoir-localized gate electrodes (gold wire and Ag/AgCl electrode) and the SWCNT-FETs. This is to a first approximation true in this work for the redox couple $K_3Fe(CN)_6/K_4Fe(CN)_6$ when the mediator concentration is restricted to 100 μM or less. Note for example the similarity of the I_{sd} vs V_g curves when 1 mM $K_3Fe(CN)_6$ and 1 mM $K_4Fe(CN)_6$ are confined to the reservoir with Ag/AgCl as the gate electrode (Figure 3C) and the similarity of the 10 and 100 μM $K_3Fe(CN)_6$ and $K_4Fe(CN)_6$ I_{sd} vs V_g curves when the mediators are located in both the reservoir and the chamber (Figure 4). Where the present observations differ most from the earlier work[17] is for concentrations of 1 mM $K_4Fe(CN)_6$ and 1 mM K_2IrCl_6 present in both the reservoir and the chamber. Incubation of the SWCNT-FET with 1 mM $K_4Fe(CN)_6$ causes the I_{sd} current to drop substantially below that observed when the mediator is confined to the reservoir for both the gold wire and the Ag/AgCl gate electrodes (Figures 3B, 3D, and 4A). The most likely interpretation for this observation is that the SWCNT-FET is being reduced by 1 mM $K_4Fe(CN)_6$ during gating with the rate of electron transfer increasing as the chemical potential difference between the nanotube and the redox mediator increases with decreasing gate voltage (more negative V_g). At lower mediator concentrations ($\leq$100 μM) the electron-transfer rate is too slow to significantly impact the I_{sd} vs V_g curves (Figure 4). This interpretation is consistent with a recent theoretical description of nanotube gating by Heller et al.[19] in which the electronic states of the valence band are increasingly emptied as the gate voltage is swept to negative potentials, promoting electron transfer from filled electronic states of the reductant to unfilled electronic states of the nanotube.

Smaller effects are observed (Figure 4) in the opposite direction for 1 mM $K_3Fe(CN)_6$ (small increase in I_{sd}), probably because of the limited ability of this relatively weak oxidant to oxidize the nanotubes. A far greater effect is observed (Figure 5) upon incubation of the SWCNT-FETs with 100 μM K_2IrCl_6, which causes the I_{sd} current to rise substantially above that observed when the mediator is confined to the reservoir only for both the gold wire (not shown) and the Ag/AgCl gate electrodes. This oxidant is capable of nearly complete bleaching of the E11 optical transitions in (6,5) carbon nanotubes, the midpoint potential of which was estimated at 800 mV.[11] The oxidation of the nanotubes by K_2IrCl_6, is so favorable (E_m = 867mV vs NHE)[28] that the minimum conductance is substantially shifted to more positive gate voltages and remains well above the minimum measured in the absence of redox mediator. In contrast to the effect of $K_4Fe(CN)_6$, the influence of K_3IrCl_6 on the SWCNT-FET conductance is quite small, presumably because of the highly unfavorable driving force for oxidation of K_3IrCl_6, even at negative gate voltages.

The effects of the redox mediators on the electronic properties of the SWCNT-FETs are consistent with the solution redox behavior of suspended SWCNTs. The nanotubes undergo reversible oxidation and reduction with the $K_3Fe(CN)_6/K_4Fe(CN)_6$ and K_2IrCl_6/K_3IrCl_6 redox couples (Figure 1 and refs 11 and 12) altering the extent to which the electronic states of the valence band are filled. This is equivalent to changing the concentration of the p-type charge carriers in the nanotubes, increasing upon oxidation. The increase in the concentration of p-type charge carriers is detectable as an increase in p-type conductance in the SWNT-FETs and is most marked for K_2IrCl_6. In addition, the redox mediators respond through electron transfer to changes in the oxidation state (chemical potential) of the SWCNTs during gating, temporizing the changes in conductance that would otherwise be seen in the absence of the redox mediator.

A comparison of the buffer I_{sd} vs V_g curves in Figures 3A and 3B shows that gating by the surface gate electrode (SG) produces an approximately 2-fold lower transconductance ($\Delta I_{sd}/\Delta V_g$) than does the gold wire. In the former case, the similarity in size of SG and the source and drain electrodes produces a potential drop of nearly equal amplitude at the gate/liquid and at the source-drain-nanotube/liquid interfaces. In the case of the gold wire, the potential drop occurs almost exclusively at the source-drain-nanotube/liquid interface owing to the much larger ($\sim$3000-fold) surface area of the gate electrode. The nearly 2-fold lower potential drop at the source-drain-nanotube/liquid interface with SG gating halves the interfacial ionic accumulation at a given V_g, halving the effective device transconductance. It is, therefore, advantageous to use a large surface area gate electrode (relative to that of the source and drain electrodes) to maximize device sensitivity.

The sensitivity of the SWCNT-FETs to changes in solution redox potential is demonstrated in Figure 6 where they are shown to be able to detect picomolar concentrations of the redox enzyme laccase through oxidation of its high reduction potential substrate, 10-(2-hydroxyethyl)phenoxazine (E_m = 773 mV vs NHE).[31] The conductance of the device varies linearly in time with substrate oxidation. In addition, the rate of change of device conductance is a linear indicator of enzyme concentration over at least 2 orders of magnitude. The sensitivity of the method to laccase concentration is comparable to that of a colorimetric assay in the presence of ABTS (2,2′-azinobis(3-ethylbenzthiazolinesulfonate), E_m = 680 mV,[33] $\epsilon_{436nm} = 2.93 \times 10^4$ M^{-1} cm^{-1} [34]) another redox substrate of laccase, the oxidation of which is also detectable in the electronic assay (not shown). However, considering that the electronic assay can be conducted in microliter and sub-microliter volumes (4.4 μL in the present case), the assay is orders of magnitude more sensitive than the colorimetric assay in terms of numbers of enzyme molecules detected. We have also been able to sense target biomolecules, the presence of which results in the binding of laccase to the surface of the silica chips, producing a highly sensitive detection method for biological analytes including DNA[16] (also manuscript in preparation).

(33) Palmore, G. T. R.; Kim, H.-H. *J. Electroanal. Chem.* **1999**, *464*, 110−117.
(34) Gelo-Pujic, M.; Kim, H.-H.; Butlin, N. G.; Palmore, G. T. R. *Appl. Environ. Microbiol.* **1999**, *65*, 5515−5521.

Conclusions

The conductance of liquid-gated SWCNT-FETs is modulated (1) by the solution electrostatic potential, poised by the chemical potential of a redox couple interacting with a gold gate electrode and (2) by the ability of the redox couple to oxidize and reduce the nanotubes. Such modulation is observed over a very broad range of redox potentials, demonstrated here for the redox couples $K_3Fe(CN)_6/K_4Fe(CN)_6$ (E_m = 0.365 v vs NHE) and K_2IrCl_6/K_3IrCl_6 (E_m = 0.867 V vs NHE). Electron transfer between the redox couple and the nanotubes mirrors nanotube oxidation and reduction observed through the optical absorbance spectra of the nanotubes. The SWCNT-FETs are shown to linearly detect the enzyme activity of the blue copper oxidase, laccase, varied over 2 orders of magnitude of enzyme concentration in the picomolar range.

Acknowledgment. The authors gratefully acknowledge useful discussions with Anand Jagota, Tian Tang, Ming Zheng, Timothy Gierke, and Lisa Larrimore and the reviewers' helpful suggestions. The authors also thank Xueping Jiang for her gift of 10-(2-hydroxyethyl)phenoxazine and Joseph Menezes for providing AFM images. This paper is contribution number 8730 from Central Research and Development of E. I. du Pont de Nemours & Co.

JA075131F